Fuel Processing Technology 194 (2019) 106115

Contents lists available at ScienceDirect

Fuel Processing Technology

journal homepage: www.elsevier.com/locate/fuproc

Potassium capture by coal fly ash: K_2CO_3, KCl and K_2SO_4

Guoliang Wang[a,*], Peter Arendt Jensen[a], Hao Wu[a], Flemming Jappe Frandsen[a], Yashasvi Laxminarayan[a], Bo Sander[b], Peter Glarborg[a]

[a] Department of Chemical and Biochemical Engineering, Technical University of Denmark, Søltofts Plads, Building 229, DK-2800 Kgs. Lyngby, Denmark
[b] Ørsted Bioenergy & Thermal Power A/S, Kraftværksvej 53, 7000 Fredericia, Denmark

ARTICLE INFO

Keywords:
Coal fly ash
Potassium capture
Biomass combustion
Additive
K_2CO_3
KCl

ABSTRACT

The potassium capture behavior of two coal fly ashes at well-controlled suspension-fired conditions was investigated through entrained flow reactor (EFR) experiments and chemical equilibrium calculations. The impact of local reaction conditions, i.e., the type of K-salts (K_2CO_3, KCl or K_2SO_4), K-concentration in flue gas (molar K/(Al + Si) ratio in reactants), reaction temperature, and coal ash type on the reaction was studied. The results show that the K-capture level of coal fly ash at a K-concentration of 500 ppmv (K/(Si + Al) = 0.481) was considerably lower than the equilibrium data as well as the measured K-capture level of kaolin. However, at 50 ppmv K (with a molar K/(Si + Al) ration of 0.048), no obvious difference between kaolin and coal fly ash was observed in this work. Comparison of results for different K-species showed that coal fly ash captured KOH and K_2CO_3 more effectively than KCl and K_2SO_4. Additionally, a coal fly ash with higher content of Si and a lower melting point captured KCl more effectively than the reference coal fly ash.

1. Introduction

Biomass suspension-combustion has a higher electrical efficiency and higher load-flexibility compared to traditional grate-fired boilers, but the ash-related problems, including deposition, corrosion and SCR catalyst deactivation, may be more severe [1] than that in grate-fired boilers [2–10], due to a higher concentration of fly ash in the flue gas [6]. Potassium originating from biomass is the primary cause for the ash-related problems. Potassium may be present as KOH, KCl, K_2SO_4 in the flue gas or other forms depending on the fuel composition, ash transformation chemistry, combustion conditions, etc. [3]. In the combustion of woody biomass which contains relatively lower chlorine and sulfur, potassium exists in the flue gas in the boiler chamber mainly as gaseous KOH [11,12]. When firing straw or other chlorine-rich biomass, chlorine facilitates the release of potassium, and KCl becomes the main K-species in the high temperature flue gas [8,13]. Apart from accelerating deposit formation and SCR catalyst deactivation, severe corrosion is also attributed to KCl [14–18]. When firing bio-fuels containing sulfur, another K-compound, K_2SO_4, can be formed [9]. The binary system of KCl and K_2SO_4 may melt at temperatures as low as 690 °C [19], forming a sticky surface on super-heaters and boiler surfaces, which results in accelerated fouling and slagging.

Various technologies have been developed to overcome these ash-related problems in biomass-fired boilers, including the use of additives [20–28], co-firing [29], leaching [30–33], and application of anti-corrosion coating or materials [34,35]. Kaolin and coal fly ash are effective additives which can chemically capture K-species forming K-aluminosilicates with higher melting points.

Coal fly ash is the only additive that has been commercially utilized in full-scale biomass suspension-fired boilers for K-capture [12,36]. In a full-scale boiler measuring campaign conducted by Wu and co-workers [36], the influence of the addition of coal fly ash on the transformation of potassium, the deposition behavior, the deposit composition and the formation of sub-micrometer aerosols was systematically investigated [12,36]. The formation of aerosols was significantly suppressed, and the composition of the aerosols changed from K-S-Cl rich to Ca-P-Si rich [12] with the addition of coal fly ash. The large outer deposit changed from K-Ca-Si rich to Si-Al rich, resulting in an easier and more frequent removal of the deposits [36]. However, due to the complexity of full-scale boiler combustion and the inevitable variation of conditions (bulk chemistry of fuel, load of boiler, etc.), it is almost impossible to conduct well-controlled quantitative studies on the K-capture reaction of coal fly ash in full-scale boilers.

Some lab-scale experiments have been carried out to understand the K-capture reaction systematically [37,38]. Zheng et al. [37] studied the KCl capture behavior of coal fly ash pellets in a lab-scale fixed bed reactor, where two types of coal ash were utilized: bituminous coal ash and lignite coal ash. The influences of parent coal type, the reaction

* Corresponding author.
E-mail address: guow@kt.dtu.dk (G. Wang).

https://doi.org/10.1016/j.fuproc.2019.05.038
Received 13 March 2019; Received in revised form 26 May 2019; Accepted 26 May 2019
Available online 12 June 2019
0378-3820/

temperature, and the K-concentration on the reaction were investigated. The results were also compared with that of kaolin [39], showing that bituminous coal ash with a high content of Al and Si behaved similarly to kaolin and captured KCl effectively. However, the lignite coal ash pellets, which were rich in Ca and Mg, only captured negligible amounts of potassium [37].

In another fixed bed reactor study, Liu et al. [38] investigated the KCl capture reaction by bituminous coal fly ash (70–100 μm) which were paved in a stainless steel wires holder [38]. The impact of reaction temperature, KCl-concentration and the reaction atmosphere was investigated. The results indicated that 900 °C was the optimal K-capture temperature for the investigated coal fly ash. In addition, a reducing atmosphere and the presence of water vapor promoted the K-capture capability of the coal fly ash [38].

Through these fixed bed studies, important data on K-capture by coal fly ash were obtained. However, the reaction conditions in the fixed bed reactors are obviously different from those in full-scale suspension-fired boilers [37]. In the fixed bed reactors, coal ash was usually in the form of pellets, flakes, piles or paved in holders [37,40,41], causing the reaction with gaseous K-species to be limited by internal diffusion. In suspension-fired boilers, coal ash particles are well-dispersed in the flue gas, having a size smaller than 100 μm, and the controlling mechanism can be quite different. The K-capture reaction under suspension-fired conditions can be limited by thermal equilibrium, mass transfer, or chemical kinetics. Additionally, local reaction temperature, gas atmosphere, additive particle size, additive composition and reaction time also impact upon the K-capture reaction by coal fly ash [37,42,43]. However, knowledge on the K-capture reaction of coal ash is limited, and quantitative experimental results on K-capture by coal fly ash at suspension-fired conditions are still not available. Understanding the reaction as well as its relation to local parameters is desirable to achieve an optimal performance of added coal fly ash and model development.

The objective of this work is to investigate quantitatively the reaction between coal fly ash and K-species at suspension-fired conditions. The impacts of coal ash type, ash particle size, K-species type, K-concentration, and reaction temperature on the K-capture reaction were investigated. This paper is the second one of a series of two papers studying the potassium capture reaction with coal fly ash. The first paper focused on the KOH capture reaction by coal fly ash [44], and the present paper addresses the reaction of coal fly ash with KCl, K_2CO_3 and K_2SO_4.

2. Experimental

2.1. Materials

Two types of coal fly ashes were utilized in this study. One was from unit 2 of Asnæsværket Power Plant Denmark, and it was named as ASV2CFA. The other ash sample was from Amager Power Plant and it was named as AMVCFA. Both coal fly ashes were sieved to 0–32 μm, and the sieved samples were named as ASV2CFA0-32 and AMVCFA0-32, respectively. The characteristics of the ash samples are listed in Table 1. Both coal fly ashes have a high content of Al and Si. The molar ratio (K + Na)/(Al + Si) of ASV2CFA0-32 and AMVCFA0-32 was 0.02, and 0.07, respectively. Both values are relatively low, indicating that there was a large fraction of Al and Si available for the K-capture reaction.

One difference between the two coal fly ashes was the alkali metal content. The concentration of (K + Na) in AMVCFA0-32 was about 3.0 wt%, while it was as low as 1.1% in ASV2CFA0-32. Alkali elements generally stay in the form of alkali-aluminosilicates in coal ash. A higher content of alkali elements in coal ash may thus reduce the availability of Al and Si for alkali-capture. Another difference was that, the Si/Al molar ratio of ASV2CFA0-32 was around 1.5, while the ratio for AMVCFA0-32 was 2.2. Usually, Si is present in the form of mullite, quartz or other amorphous species in coal ash. A relatively higher Si or lower Al content usually implies a lower content of mullite, which is considered as a crucial mineral phase in coal ash for K-capture reaction forming K-aluminosilicate [36,37,42].

Table 1
Characteristics of the coal fly ashes.

Name	ASV2CFA0-32	AMVCFA0-32
Particle size (μm)	0–32	0–32
D_{50} (μm)	10.20	8.42
O (wt% dry base)	46.60	49.92
S (wt% dry base)	0.26	0.23
P (wt% dry base)	0.64	0.30
Si (wt% dry base)	22.00	25.00
Al (wt% dry base)	14.00	11.00
Fe (wt% dry base)	2.90	4.30
Ca (wt% dry base)	4.50	4.10
Mg (wt% dry base)	0.97	1.40
Na (wt% dry base)	0.27	0.92
K (wt% dry base)	0.87	2.10
Ti (wt% dry base)	0.88	0.53
BET surface area (m^2/g)	8.04	3.18
Deformation temperature (°C)	1280	1200
Hemisphere temperature (°C)	1390	1290
Flow temperature (°C)	1440	1380

Among the alkaline earth metal elements, the content of Ca in AMVCFA0-32 was slightly lower than that of ASV2CFA0-32, while Mg was slightly higher. Ca is primarily present in coal ash as lime, anhydrite or calcite [45,46], and it can also exist together with Mg as CaMg-silicate [47,48]. Therefore, Ca and Mg may also affect the availability of Al and Si, but to a lower extent. In summary, the relatively lower content of Al and higher content of K and Na would be expected to weaken the K-capture ability of AMVCFA0-32.

In addition to Al and Si, S may also constitute a protective element in coal fly ash, since it can react with KCl or KOH forming less corrosive potassium sulfate [36]. However, the concentration of S in the two selected ashes was very low, around 0.25%, and may not play a key role in the K-capture reaction in this study.

XRD results show that quartz (SiO_2) and mullite ($3Al_2O_3{\cdot}2SiO_2$) exist in both two coal fly ashes as the main mineral phases. However, no crystalline species containing alkali or alkaline earth metal elements were detected, implying either that the small amount of Na, K, Ca and Mg detected by ICP-OES stay in the form of amorphous species, or that the concentrations were too low to be detected.

Additionally, the melting points (deformation temperature, hemisphere temperature and flow temperature) of the two coal fly ashes were also analyzed according to ISO540:2008 (Hard coal and coke - Determination of ash fusibility) in an oxidizing atmosphere. The results are listed in Table 1, and it revealed that and the melting points of AMVCFA0-32 are lower than that of ASV2CFA0-32.

2.2. Experimental methods

The DTU Entrained Flow Reactor (EFR) was employed in the experimental work. Detailed information about the reactor is available elsewhere [27,39]. The experimental conditions are summarized in Table 2. In series A of Table 2, to study the influence of KCl concentration, the concentration of coal fly ash in flue gas was kept constant, while the KCl concentration in flue gas was varied from 50 ppmv to 750 ppmv. In series (B) and (C), the KCl-concentration was kept constant, while the reaction temperature was changed from 800 to 1450 °C, to investigate the influence of reaction temperature. ASV2CFA0-32 and AMVCFA0-32 were utilized in series B and C to compare the KCl capture behavior of the two ashes. The K_2CO_3 and K_2SO_4 capturing behavior by coal fly ash at different temperatures was investigated in series (D) and (E).

The solid products collected from the EFR experiments were

Table 2
Experimental conditions of K-capture experiments using coal fly ashes in the EFR.

Experimental series	K-species	Additives	Temp./°C	Gas residence time/s	K in gas /ppmv	K/(Al + Si)
(A) KCl-capture by ASV2CFA0-32 (impact of **K-concentration**)	KCl	ASV2CFA0-32	1300	1.2	50* 250 500* 750	0.048 0.240 0.481 0.961
(B) KCl-capture by ASV2CFA0-32 (impact of **temperature**)	KCl	ASV2CFA0-32	800 900 1100 1300 1450	1.2	50, 500	0.048, 0.481
(C) KCl-capture by AMVCFA0-32 (impact of **temperature**)	KCl	AMVCFA0-32	800 900 1100 1300 1450	1.2	500	0.481
(D) K_2CO_3-capture by ASV2CFA0-32 (impact of **temperature**)	K_2CO_3	ASV2CFA0-32	800 900 1300	1.2	500	0.481
(E) K_2SO_4-capture by ASV2CFA0-32 (impact of **temperature**)	K_2SO_4	ASV2CFA0-32	800 900 1300*	1.2	500	0.481

* Experiments were repeated.

analyzed with ICP-OES (Inductively Coupled Plasma Atomic Emission Spectroscopy) to obtain the elemental composition. For the ICP-OES analysis, solid samples were totally digested in acid solution or dissolved in water to determine the total content or the water-soluble content of different elements, including major elements and water soluble elements. The major elements (Al, Ca, Fe, Mg, P, S, K, Si, Na and Ti) were determined according to the Danish Standard of DS/EN 15290 (Solid Biofuels - Determination of Major Elements). The concentration of water-soluble elements (K and Cl) was analyzed following the standard of DS/EN ISO 16995 (Solid Biofuels- Determination of water soluble Chloride, Sodium and Potassium). Additionally, XRD (X-ray Diffraction) analysis was employed to get the mineralogical composition of solid products. The XRD spectra were obtained with a Huber diffractometer, and the main crystalline phases were identified with the JADE 6.0 software package (MDI Livermore, CA) and the diffraction database of PDF2-2004.

To quantify the K-capture reaction by coal fly ash, two parameters have been defined: K-conversion (X_K) and K-capture level (C_K). X_K is the percentage (%) of fed K-species chemically captured by solid additive (coal fly ash) forming water-insoluble K-aluminosilicates. C_K is the mass of potassium captured by 1 g of additive (coal fly ash) (g K/g additive). Both two parameters can be calculated based on ICP-OES results, and the detailed calculation method is available in the Appendix I of the supplementary material.

2.3. Equilibrium calculations

Equilibrium data were obtained by preforming global chemical equilibrium calculations using FactSage 7.0. The equilibrium calculation results were compared with experimental results to obtain a better understand of the experimental data. But one should note that equilibrium calculation data are obtained assuming a fully mixing of all reactants with an enough long time, which could be not reached in real experiments, and the difference of equilibrium calculation and experimental results can be partly contributed to this.

3. Results and discussion

3.1. KCl capture by coal fly ash

3.1.1. Equilibrium calculations

Equilibrium calculation results of KCl capture by ASV2CFA0-32 at 50–1000 ppmv KCl and 800–1450 °C were summarized in Table 3. Detailed results of the equilibrium calculations are provided in Appendix II of the supplementary material. The results show that the type of K-aluminosilicate formed from the K-capture reaction varied with the changing KCl-concentration and the corresponding molar ratio of K/(Al + Si) in reactants. At 50 ppmv KCl (K/(Al + Si) = 0.048), sanidine ($KAlSi_3O_8$) was the main K-aluminosilicate. When the KCl concentration increased to 250 ppmv and 500 ppmv (K/(Al + Si) = 0.240 and 0.481), leucite ($KAlSi_2O_6$) was predicted to be the dominant K-aluminosilicate at 1100–1450 °C. At 800–900 °C, kaliophilite ($KAlSiO_4$) and leucite ($KAlSi_2O_6$) co-existed in the solid products. The equilibrium K-capture level (C_K) increased when the KCl concentration changed from 50 ppmv to 500 ppmv. However, when the KCl concentration was increased further to 750 and 1000 ppmv, no further increase of equilibrium C_K was observed.

3.1.2. Impact of KCl concentration

To investigate the KCl-capture behavior of coal fly ash at different KCl concentrations, experiments were conducted at 50 ppmv to 750 ppmv KCl, where the molar ratio of K/(Al + Si) in reactants changed from 0.048 to 0.721, correspondingly. The experimental results and equilibrium calculation data are compared in Fig. 1. Results for KCl-capture by kaolin from our previous study [39] were also included for comparison.

It is seen from Fig. 1, that the measured K-capture level (C_K) of ASV2CFA0-32 increased from 0.019 g K/(g additive) to 0.041 g K/(g additive), when the KCl concentration increased from 50 ppmv to 500 ppmv. Measured K-conversion (X_K) of ASV2CFA0-32 decreased from 80.0% to 17.5% correspondingly. However, when the KCl-concentration increased further to 750 ppmv and 1000 ppmv, C_K did not increase, with X_K decreased further to 11.7%. Comparing to the equilibrium calculation results, the measured C_K and X_K was considerably lower. This implied that the KCl-ASV2CFA0-32 reaction was far from

Table 3
Equilibrium calculation results of KCl capture by ASV2CFA0-32.

Input conditions	Temp. /°C	K-species appearing	Al-conversion /%	Si-conversion /%	K-conversion (X_K) /%	K-capture (C_K) /(g K/g additive)
50 ppmv KCl, K/(Al+Si) =0.048	800	100 % $KAlSi_3O_8$	12	24	100	0.023
	900	100 % KAlSi3O_8	12	24	100	0.023
	1100	99 % $KAlSi_3O_8$ + 1 % KCl	12	24	99	0.023
	1300	97 % $KAlSi_3O_8$ + 3 % KCl	12	23	97	0.023
	1450	92 % $KAlSi_3O_8$ + 7 % KCl + 1 % KOH	11	22	92	0.021
250 ppmv KCl, K/(Al+Si) =0.240	800	95 % $KAlSi_2O_6$ + 5 % KCl	57	77	95	0.111
	900	94 % $KAlSi_2O_6$ + 6 % KCl	57	76	94	0.110
	1100	89 % $KAlSi_2O_6$ + 11 % KCl	54	72	89	0.104
	1300	84 % $KAlSi_2O_6$ + 16 % KCl	50	68	84	0.098
	1450	81 % $KAlSi_2O_6$ + 18 % KCl + 1 % KOH	49	66	81	0.095
500 ppmv KCl, K/(Al+Si) =0.481	800	6 % $KAlSiO_4$ + 51 % $KAlSi_2O_6$ + 40 % KCl	69	88	57	0.134
	900	55 % $KAlSi_2O_6$ + 45 % KCl	66	88	55	0.128
	1100	47 % $KAlSi_2O_6$ + 53 % KCl	57	76	47	0.110
	1300	46 % $KAlSi_2O_6$ + 53 % KCl + 1 % KOH	56	75	46	0.109
	1450	45 % $KAlSi_2O_6$ + 54 % KCl + 1 % KOH	54	72	45	0.104
750 ppmv KCl, K/(Al+Si) =0.721	800	33 % $KAlSiO_4$ + 19 % $KAlSi_2O_6$ + 46 % KCl	95	72	52	0.184
	900	3 % $KAlSiO_4$ + 35 % $KAlSi_2O_6$ + 63 % KCl	68	73	37	0.131
	1100	33 % $KAlSi_2O_6$ + 67 % KCl	59	65	33	0.114
	1300	31 % $KAlSi_2O_6$ + 68 % KCl + 1 % KOH	56	62	31	0.109
	1450	31 % $KAlSi_2O_6$ + 67 % KCl + 2 % KOH	56	62	31	0.109
1000 ppmv KCl, K/(Al+Si) =0.961	800	29 % $KAlSiO_4$ + 19 % $KAlSi_2O_6$ + 57 % KCl	100	87	41	0.193
	900	16 % $KAlSiO_4$ + 19 % $KAlSi_2O_6$ + 65 % KCl	84	87	35	0.162
	1100	25 % $KAlSi_2O_6$ + 75 % KCl	60	81	25	0.116
	1300	25 % $KAlSi_2O_6$ + 75 % KCl + 1 % KOH	56	75	23	0.109
	1450	23 % $KAlSi_2O_6$ + 75 % KCl + 2 % KOH	56	75	23	0.109

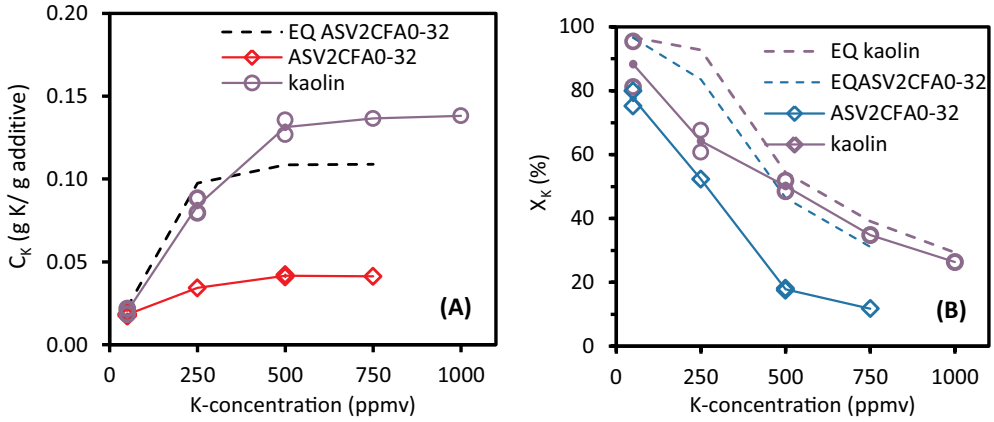

Fig. 1. K-capture level (C_K) and K-conversion (X_K) of KCl capture by ASV2CFA0-32 at 50–750 ppmv KCl (molar ratio of K/(Al + Si) changed from 0.048 to 0.721). Reaction temperature was 1300 °C; the gas residence time was 1.2 s. Experimental data of KCl capture by kaolin from our previous study [39] and equilibrium calculation data of KCl capture by ASV2CFA0-32 were included for comparison.

reaching chemical equilibrium probably due to internal diffusion limitations of KCl.

Comparing the C_K and X_K of ASV2CFA0-32 with kaolin [39] in Fig. 1, at 250 ppmv KCl and above, the experimental C_K and X_K of ASV2CFA0-32 were remarkably lower than that of kaolin [39]. The lower BET surface area (8.04 m^2/g) and the relatively bigger particle size (D_{50} = 10.20 μm) of ASV2CFA0-32 compared with kaolin (BET surface area = 12.70 m^2/g, D_{50} = 5.47 μm) was one possible reason; another possible reason being the lower reactivity of mullite in coal fly ash towards potassium, compared to kaolinite [37]. At 50 ppmv KCl (K/(Al + Si) in reactants was 0.048), the measured C_K and X_K of ASV2CFA0-32 were comparable to those of kaolin [39]. The results indicated that at low K-concentrations (50 ppmv) or low K/(Al + Si) molar ratio (0.048), which is representative for the gaseous potassium level in practical wood suspension-fired plants [36,49–51], the K-capture capacity of kaolin and coal fly ash is similar. This is probably because at lower K/(Al + Si), the mullite in the surface layer of coal fly ash particles is probably sufficient for capturing the low amount of potassium, therefore the reaction is less influenced by the internal diffusion of KCl.

The XRD results of water-washed KCl-reacted ASV2CFA0-32 are shown in Fig. 2. It shows that the XRD spectrum of 50 ppmv KCl-reacted ash is almost identical as that of coal ash without K feeding, and no crystalline K-aluminosilicate was detected, although sanidine ($KAlSi_3O_8$) was predicted by the equilibrium calculations (Table 3) and some water-insoluble potassium was detected by ICP-OES analysis. This is probably because K-aluminosilicate products existed in amorphous phase or its content was too low to be detected. Leucite ($KAlSi_2O_6$) was detected both in the 250 ppmv and 500 ppmv KCl-reacted ash samples. This agrees with the equilibrium prediction shown in Table 3. Additionally, the types of K-aluminosilicate detected also agreed with what was observed in KCl-kaolin reaction in our previous study [39]. Notably, in addition to K-aluminosilicate, mullite ($3Al_2O_3{\cdot}2SiO_2$) and quartz (SiO_2) were also detected in all the KCl-reacted ash samples, indicating that some mullite and quartz originating from the parental coal fly ash remained unreacted. This is presumably the reason why the measured K-capture level (C_K) of ASV2CFA0-32 was remarkably lower than the equilibrium prediction.

3.1.3. Impact of reaction temperature

The K-capture level (C_K) and K-conversion (X_K) of KCl capture by ASV2CFA0-32 and AMVCFA0-32 at different temperatures are shown in Fig. 3 and Fig. 4, respectively. For ASV2CFA0-32, experiments were conducted at both 50 ppmv and 500 ppmv KCl. For AMVCFA0-32, experiments were only conducted with a KCl concentration of 500 ppmv.

As shown in Fig. 3(A) and (B), at 50 ppmv KCl (K/(Al + Si) = 0.048), the measured C_K and X_K of ASV2CFA0-32 were close to the equilibrium calculation data and no obvious change of C_K was observed within the studied temperature range (800–1450 °C). C_K was around 0.018 g K/(g additive), with about 80% of the potassium fed captured by coal fly ash.

Fig. 3(C) and (D) show that, at 800 °C and 500 ppmv KCl (K/(Al + Si) = 0.481), the experimental C_K is fairly low (0.015 g K/(g additive)). However, when the reaction temperature increased to 900 °C,

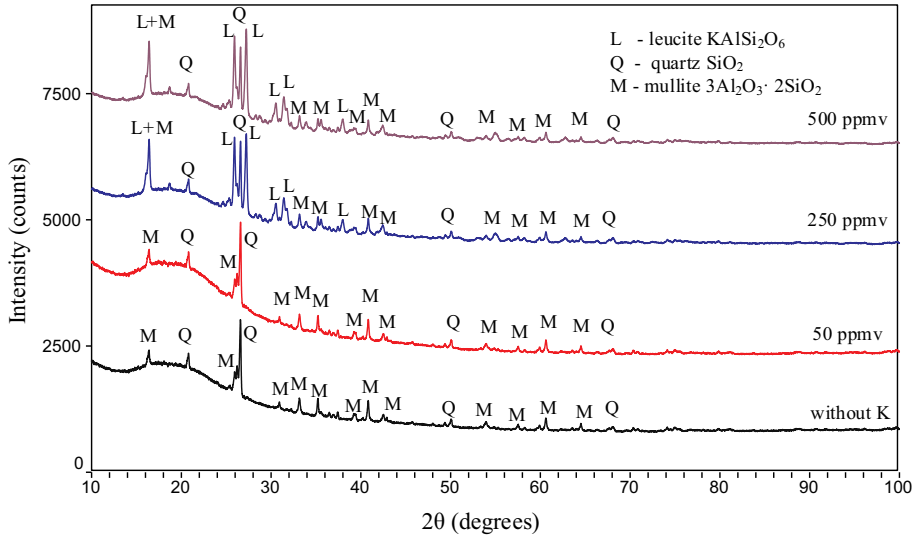

Fig. 2. XRD spectra of water-washed KCl-reacted ASV2CFA0-32 at 50 ppmv, 250 ppmv and 500 ppmv KCl. The reaction temperature was 1300 °C. The molar ratio of K/(Al + Si) in the reactants changed from 0.048 to 0.481. The gas residence time was 1.2 s. XRD spectrum of coal fly ash without K feeding was also included for comparison.

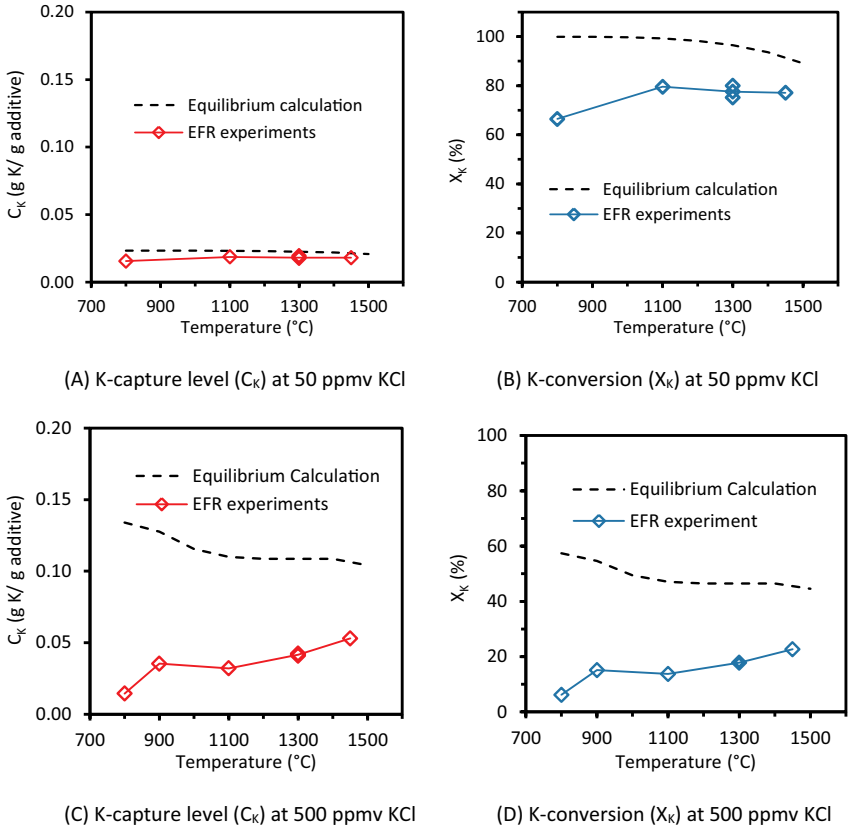

Fig. 3. K-capture level (C_K) and K-conversion (X_K) of KCl-capture by ASV2CFA0-32 at 800–1450 °C. KCl-concentration was 50 ppmv (molar ratio of K/(Al + Si) = 0.048) in (A) and (B), and 500 ppmv (molar ratio of K/(Al + Si) = 0.481) in (C) and (D). The gas residence time was 1.2 s. Equilibrium calculation results are included for comparison.

the experimental C_K increased significantly to 0.035 g K/(g additive). In the temperature range 900–1100 °C, no significant change of C_K and X_K was observed. We believe that this is because, at 800 °C, the KCl-coal fly ash reaction was probably kinetically controlled, and it was less kinetically influenced at 900–1100 °C. As the reaction temperature increased further to 1300 and 1450 °C, C_K increased gradually to 0.053 g K/(g additive). However, the experimental C_K and X_K were both obviously lower than the equilibrium predictions. Noticing the vaporization degree of KCl (500 ppmv) at different temperatures from 800 to 1450 °C in the EFR was similar (95.4–99.7%) [39]. The increase of C_K at 900–1450 °C, especially at 1300 °C and 1450 °C, is probably due to the melting of coal ash particles (deformation temperature of ASV2CFA0-32 was 1280 °C), which enhanced the KCl diffusion inside the particle (D_{50} = 10.20 μm). A similar phenomenon was observed in the KCl capture experiments using AMVCFA0-32, as discussed below.

Another interesting result in Fig. 3 is that, at 800 °C, C_K at 500 ppmv KCl (0.015 g K/(g additive)) is comparable to that at 50 ppmv KCl (0.014 g K/(g additive)). It shows that, at 800 °C, increasing the KCl-concentration from 50 to 500 ppmv did not elevate the amount of potassium captured by coal fly ash under the studied condition. This is probably because the reaction at 800 °C was kinetically controlled and the KCl concentration did not to a large degree influence the reaction.

The experimental C_K and X_K for KCl-capture by AMVCFA0-32 are shown in Fig. 4 (A) and (B). The trend of C_K and X_K of AMVCFA0-32 at different temperatures was similar to that of ASV2CFA0-32. At 800 °C, C_K was as low as 0.015 g K/(g additive), and it increased to around 0.030 g K/(g additive) at 900 and 1100 °C. When the temperature increased further to 1300 and 1450 °C, C_K increased considerably to 0.069 g K/(g additive).

The experimental C_K for KCl capture by bituminous coal fly ash pellets (diameter of 1.5 mm in a fixed bed reactor) from literature [37] is included in Fig. 4 (A) for comparison. The KCl concentration in the fixed bed reactor was 1000 ppmv, and the residence time was 1 h, i.e., much longer than that in the EFR (1.2 s) of this study. It is seen that C_K in the fixed bed reactor from literature was considerably higher than that in the EFR at 800–1100 °C. This is because the longer residence

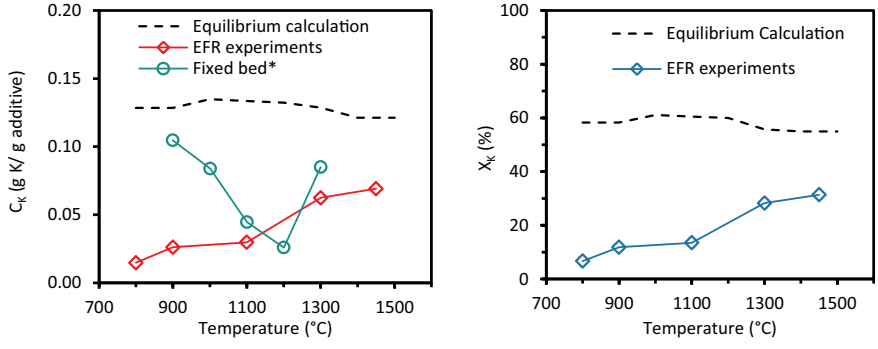

Fig. 4. K-capture level (C_K) and K-conversion (X_K) of KCl capture by AMVCFA0-32 at different temperatures (800–1450 °C). KCl concentration was 500 ppmv with molar ratio of K/(Al + Si) = 0.481 in reactants. The gas residence time was 1.2 s. Equilibrium calculation results and fixed bed reactor data* (bituminous coal ash pellets with diameter of 1.5 mm, 1100 °C, 1000 ppmv KCl, residence time was 1 h) calculated from literature [37] are included for comparison.

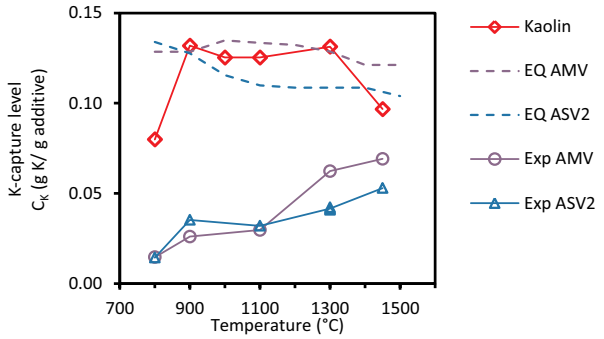

Fig. 5. Comparison of C_K of KCl capture by ASV2CFA0-32, AMVCFA0-32 and kaolin [39] at different temperature. KCl-concentration was 500 ppmv with molar ratio of K/(Al + Si) = 0.481, gas residence time was 1.2 s. Equilibrium calculation data of KCl capture by ASV2CA0-32 and AMVCFA0-32 were included for comparison.

time in the fixed bed reactor favored the reaction and more Al and Si from coal fly ash participated in the KCl capture reaction. However, at 1300 °C, the C_K in fixed bed and EFR became comparable despite the difference in residence time and KCl concentration. Possibly, this is because the melting of the ash particles at high temperature (1300 °C and 1450 °C) made the reaction in the EFR less diffusion-influenced.

3.1.4. Impact of coal fly ash type

The experimental C_K of the two coal ashes (ASV2CFA0-32 and AMVCFA0-32) as well as that of kaolin from our previous study [39] are compared in Fig. 5. The equilibrium calculation data of KCl capture by the two coal fly ashes were also included. Below 1100 °C, C_K and X_K of ASV2CFA0-32 and AMVCFA0-32 were similar, whereas at 1300 °C and 1450 °C, AMVCFA0-32 captured KCl more effectively than ASV2CFA0-32, despite its higher content of K and Na. One possible explanation is that the melting point of AMVCFA0-32 is lower than that of ASV2CFA0-32 as shown in Table 1. The melting of the ash particles presumably facilitates internal diffusion of KCl. Similar phenomena, that the K-capture amount by coal fly ash increased at 1200 °C and above, was observed by Zheng in a fixed bed study of KCl capture by coal fly ash pellets [37]. Another possible reason is that the Si concentration in AMVCFA0-32 is higher than that in ASV2CFA0-32. The higher Si content facilitated the formation of leucite ($KAlSi_2O_6$) (K:Al:Si = 1:1:2) in the KCl-coal fly ash reaction. A higher C_K of AMVCFA0-32 was observed both in the equilibrium calculations and the EFR experiments at 1300 °C and 1450 °C.

3.2. K_2CO_3 capture by coal fly ash

3.2.1. Equilibrium calculation

Equilibrium calculations of K_2CO_3 capture by ASV2CFA0-32 were conducted with a K_2CO_3 concentration of 250 ppmv (K-concentration in flue gas was 500 ppmv), and reaction temperatures changing from 500 °C to 1800 °C. The equilibrium calculation results are summarized in Table 4, and detailed data can be found in Appendix II of the Supplementary material.

The equilibrium calculation results generally agreed with the prediction for KOH-capture by ASV2CFA0-32 in our previous study [44]. At 250 ppmv K_2CO_3 (K/(Al + Si) = 0.481) and 800–1300 °C, kaliophilite ($KAlSiO_4$) was predicted to be the dominant K-aluminosilicate in products, together with some (leucite) $KAlSi_2O_6$. At 1450 °C, leucite ($KAlSi_2O_6$) was present as the dominant K-aluminosilicate product. The equilibrium C_K and X_K was constant at 800–1300 °C, and a decreased C_K was predicted at 1450 °C.

3.2.2. Impact of reaction temperature

The measured C_K and X_K of K_2CO_3 capture by ASV2CFA0-32 are

Table 4
Summary of the equilibrium calculation results of K_2CO_3 capture by ASV2CFA0-32.

Input conditions	Temp. /°C	K-species appearing	Al-conversion /%	Si-conversion /%	K-conversion (X_K) /%	K-capture (C_K) /(g K/g additive)
250 ppmv K_2CO_3, K/(Al+Si) = 0.481	800	73 % $KAlSiO_4$ + 10 % $KAlSi_2O_6$	100	76	83	0.194
	900	71 % $KAlSiO_4$ + 12 % $KAlSi2O_6$ + 2 % KOH	100	77	83	0.194
	1100	55 % $KAlSiO_4$ + 28 % $KAlSi_2O_6$ + 15 % KOH	100	90	83	0.194
	1300	55 % $KAlSiO_4$ + 28 % $KAlSi_2O_6$ + 17 % KOH	100	90	83	0.194
	1450	57 % $KAlSi_2O_6$ + 42 % KOH	69	92	57	0.133

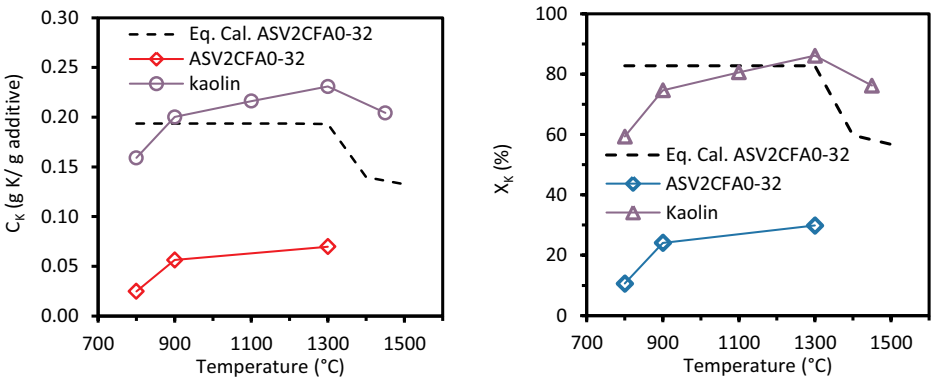

Fig. 6. K-capture level (C_K) and K-conversion (X_K) of K_2CO_3 capture by ASV2CFA0-32 at 800–1300 °C. K_2CO_3 concentration was 250 ppmv (molar ratio of K/(Al + Si) = 0.481). The gas residence time was 1.2 s. Equilibrium calculation results of K_2CO_3 capture by ASV2CFA0-32, and experimental results of K_2CO_3-capture by kaolin from our previous study [39] are included for comparison.

compared to the equilibrium calculations in Fig. 6, under the conditions of 800–1300 °C, 250 ppmv K_2CO_3 and a gas residence time of 1.2 s. The experimental C_K and X_K of K_2CO_3 capture by kaolin (D_{50} = 5.47 μm) from our previous study [39] were included for comparison. We believe that at the applied temperatures (800 °C and above) K_2CO_3 decomposes to KOH that reacts with the coal fly ash.

According to our previous work, the vaporization degree of K_2CO_3 at 800–1450 °C in the EFR was similar (97.3–99.7%). However, experimental C_K (0.025 g K/(g additive)) at 800 °C was much lower than that at 900 °C (0.056 g K/(g additive)). The significant difference is probably because the reaction was kinetically controlled at 800 °C. When the reaction temperature increased to 1300 °C, C_K increased slightly to 0.070 g K/(g additive). The experimental X_K had the same trend as that of C_K, and it was below 30% throughout the whole temperature range studied.

The results also show that the experimental C_K and X_K of ASV2CFA0-32 were significantly lower than that of kaolin [39] and the data predicted by equilibrium calculations. The lower BET surface area of coal fly ash (8.04 m^2/g) than that of kaolin (12.70 m^2/g), and the bigger particle size of ASV2CFA0-32 (D_{50} = 12.70 μm) than that of kaolin (D_{50} = 5.47 μm) may cause some of the difference. Another possible reason is that the main mineral phase in ASV2CFA0-32, mullite, was less active towards K_2CO_3. Additionally, the relatively lower Al content of ASV2CFA0-32 may have contributed to the lower C_K as well.

The XRD spectra of water-washed K_2CO_3-reacted ASV2CFA0-32 at different temperatures were compared in Fig. 7. In the 1300 °C sample, kaliophilite ($KAlSiO_4$) was detected together with mullite and quartz. However, in the 800 °C and 900 °C samples, no crystalline K-aluminosilicate was detected although the ICP-OES analysis showed that the experimental C_K at 900 °C was similar as that of 1300 °C. This is probably because, at 900 °C, only amorphous K-aluminosilicate was formed, and it cannot be detected by XRD.

3.3. K_2SO_4 capture by coal fly ash

3.3.1. Equilibrium calculation

Equilibrium calculations of K_2SO_4 capture by ASV2CFA0-32 were conducted at 250 ppmv K_2SO_4 and a temperature range from 500 °C to 1800 °C. The equilibrium calculation results are summarized in Table 5. Detailed results are provided in Appendix II of the Supplementary material.

The equilibrium calculations show that at 800 °C, 900 °C and 1450 °C, leucite ($KAlSi_2O_6$) was predicted to be the dominant K-aluminosilicate product. At 1100 °C and 1300 °C, kaliophilite ($KAlSiO_4$) was predicted to be present as the main K-aluminosilicate in the product. The calculated C_K firstly increased and then decreased with the increasing temperature in the studied temperature range.

3.3.2. Impact of temperature

The experimental C_K and X_K of K_2SO_4 capture by ASV2CFA0-32 are compared with equilibrium calculations as well as the experimental C_K and X_K of K_2SO_4 capture by kaolin [39] in Fig. 8. At 800 °C, C_K of ASV2CFA0-32 was 0.013 g K/(g additive), with only 5.7% K_2SO_4 converted into K-aluminosilicate. The low conversion was partly because of an incomplete vaporization of K_2SO_4, and partly because of that the reaction was slow at 800 °C. At 900 °C and 1300 °C, C_K increased to

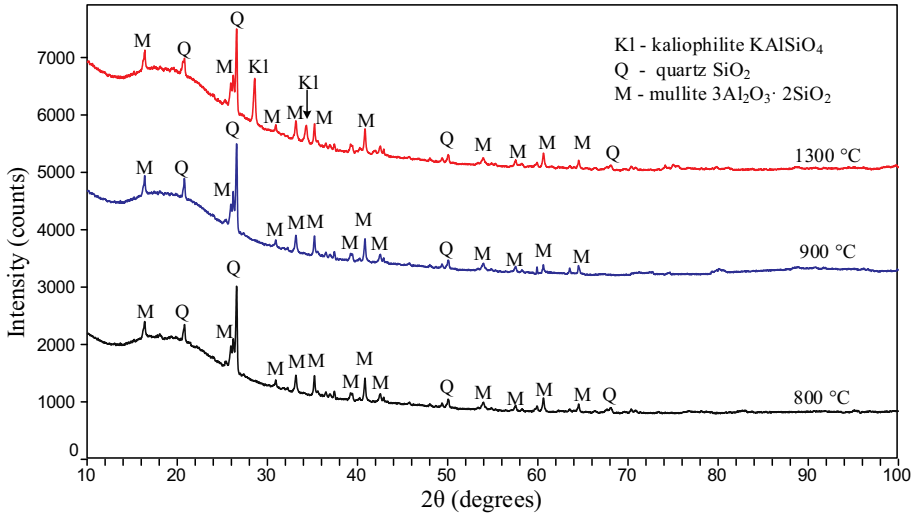

Fig. 7. XRD spectra of water-washed K_2CO_3-reacted ASV2CFA0-32. K_2CO_3 concentration in flue gas was 250 ppmv; molar ratio of K/(Al + Si) in reactants was 0.481. Gas residence time was 1.2 s.

Table 5
Summary of the equilibrium calculation results of K_2SO_4 capture by ASV2CFA0-32.

Input conditions	Temp./°C	K-species appearing	Al-conversion/%	Si-conversion/%	K-conversion(X_K)/%	K-capture (C_K)/(g K/g additive)
250 ppmv K_2SO_4, K/(Al + Si) = 0.481	800	60% $KAlSi_2O_6$ + 40% K_2SO_4	73	98	60	0.141
	900	59% $KAlSi_2O_6$ + 28% K_2SO_4	72	96	59	0.139
	1100	54% $KAlSiO_4$ + 28% $KAlSi_2O_6$ + 4% KOH	99	89	82	0.191
	1300	54% $KAlSiO_4$ + 28% $KAlSi_2O_6$ + 16% KOH	100	90	83	0.193
	1450	57% $KAlSi_2O_6$ + 42% KOH	69	92	57	0.133

0.025 g K/(g additive) and 0.037 g K/(g additive) respectively. However, similar to what was observed for KCl and K_2CO_3 capture by ASV2CFA0-32, the measured C_K and X_K of K_2SO_4 were remarkably lower than the equilibrium data. This is because the fly ash only partly reacted, with some mullite remaining unreacted in products. This was supported by the XRD results discussed below.

The XRD spectra of water-washed K_2SO_4-reacted ASV2 coal fly ash are compared in Fig. 9. At 800 °C and 900 °C, only mullite and quartz were detected in the products, with no indication of crystalline K-aluminosilicates. In the 1300 °C sample, leucite ($KAlSi_2O_6$) was the only K-aluminosilicate detected, although kaliophilite ($KAlSiO_4$) and leucite ($KAlSi_2O_6$) were predicted to co-exist by the equilibrium calculation. Similar results were observed in the K_2SO_4-kaolin reaction using in our previous study [39].

3.4. Comparison of different K-species

Reaction between ASV2CFA0-32 and different K-species (KOH, K_2CO_3, KCl and K_2SO_4) is compared in Fig. 10. The results of KOH-ASV2CFA0-32 reaction are from our previous study [44]. It shows that the K-capture level (C_K) for KOH and K_2CO_3 by ASV2CFA0-32 were very similar (0.05–0.07 g K/(g additive)). We attribute this to a rapid conversion of K_2CO_3 to KOH in the reactor followed by reaction of KOH with ASV2CFA0-32. A similar behavior was observed in our previous study where KOH and K_2CO_3 capture by kaolin was investigated [39]. The trend of C_K of K_2SO_4 capture by ASV2CFA0-32 at different temperatures generally agreed with that of KCl (C_K = 0.02–0.04 g K/(g additive)). Similar results were also seen in our previous study of KCl and K_2SO_4 capture by kaolin [39]. ASV2CFA0-32 captured KOH and K_2CO_3 more effectively than KCl and K_2SO_4 in the studied temperature range and K-concentration.

The results imply that in the case of capturing KCl or K_2SO_4, more additives may be needed to achieve a satisfactory K-capture. The reason for this is that at high temperatures the main product of the reaction with KCl or K_2SO_4, is leucite ($KAlSi_2O_6$) while the main product of reactions with KOH and K_2CO_3 is kaliophilite ($KAlSiO_4$). In addition, coal fly ash with a relatively higher content of Si seems more suitable than coal fly ash with a similar Al and Si contents for K-capture when burning Cl-rich biomass fuels.

4. Conclusions

The K-capture behavior of two coal fly ashes were studied by conducting experiments in an entrained flow reactor and doing chemical equilibrium calculations. The influence of the type of K-species, the K-concentration in flue gas (molar ratio of K/(Al + Si) in reactants), reaction temperature, as well as the type of coal fly ashes on the K-capture reaction was systematically investigated.

For KCl at 1300 °C, the K-capture level (C_K) of coal fly ashes increased from 0.02 g K/(g additive) to 0.04 g K/(g additive) when the KCl concentration increased from 50 ppmv to 500 ppmv (molar ratio of K/(Al + Si) in reactants increased from 0.048 to 0.481). However, C_K did not increase when the KCl concentration increased further to 750 ppmv (molar ratio of K/(Al + Si) = 0.721).

At 800 °C, the K-capture reaction was kinetically limited and a relatively low K-capture level (C_K) was observed for all studied K-species (KOH, KCl, K_2CO_3 and K_2SO_4). At 900 °C and up to 1450 °C, C_K generally increased with increasing reaction temperature for all the applied K-species. Possibly the melting of coal fly ash at high temperature (1300 and 1450 °C) enhanced the internal diffusion of K-species, and resulted a higher C_K values. KOH and K_2CO_3 had similar C_K levels of 0.05–0.07 g K/(g additive), and KCl and K_2SO_4 obtained C_K levels of 0.02–0.04 g K/(g additive) in the temperature range from 900 to 1450 °C (with a K-concentration of 500 ppmv, molar K/(Al + Si) ratio in reactants of 0.481, and a residence time of 1.2 s). At high temperature (1300 °C) crystalline kaliophilite ($KAlSiO_4$) was detected in K_2CO_3-

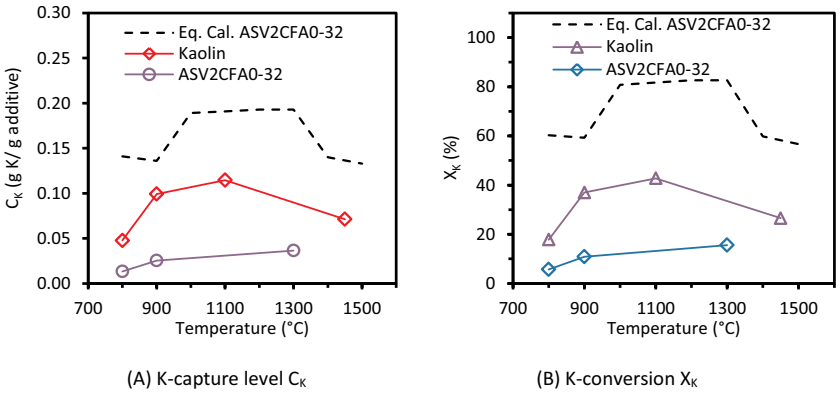

Fig. 8. K-capture level (C_K) and K-conversion (X_K) of K_2SO_4 capture by ASV2CFA0-32 at temperatures 800–1300 °C. K_2SO_4 concentration in flue gas was 250 ppmv (K-concentration in flue gas is 500 ppmv), and molar ratio of K/(Al + Si) in reactants was 0.481. The gas residence time was 1.2 s. Equilibrium calculation results of K_2SO_4 capture by ASV2CFA0-32, and experimental C_K of K_2SO_4 capture by kaolin [39] are included for comparison.

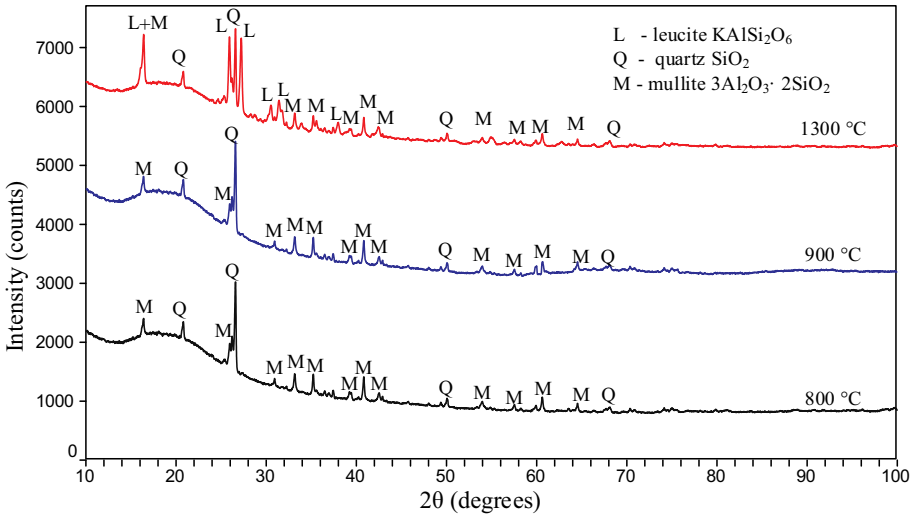

Fig. 9. XRD spectra of water-washed K_2SO_4-reacted ASV2CFA0-32 at different temperatures (800, 900 and 1300 °C). K_2SO_4 concentration was 250 ppmv; molar K/(Al + Si) ratio in reactants was 0.481. The gas residence time was 1.2 s.

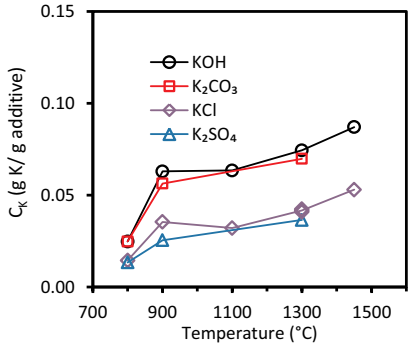

Fig. 10. Comparison of C_K of K-capture by ASV2CFA0-32 using different K-species (KOH, K_2CO_3, KCl and K_2SO_4). The K-concentration was 500 ppmv; molar K/(Al + Si) ratio in reactants was 0.481. The gas residence time was 1.2 s. *Data of KOH capture by ASV2CFA0-32 was from our previous study [44].

reacted coal fly ash, but leucite ($KAlSi_2O_6$) were detected in KCl and K_2SO_4-reacted coal fly ashes. In addition, mullite was detected in reacted coal fly ashes by XRD, showing that coal fly ash remained only partially reacted in the product samples.

The C_K and X_K levels of the two coal fly ashes were compared with that of kaolin from our previous studies [27,39]. C_K of the two coal fly ashes was obviously lower than that of kaolin at 500 ppmv K (K/(Al + Si) = 0.481). However, at 50 ppmv K (K/(Al + Si) = 0.048), which is comparable to the conditions in full-scale wood suspension-fired boilers, C_K of kaolin and coal fly ash was similar. The AMVCFA0-32 coal ash with a lower melting point and high Si content captured more KCl than ASV2CFA0-32, probably because the internal diffusion of KCl inside the AMV coal ash particles was enhanced by the melting of the coal ash particles, and the high Si content facilitated the formation of leucite ($KAlSi_2O_6$).

Based on the results obtained from this study, some guidelines on using additives in full-scale PF-boilers are summarized below.

- The composition of coal fly ash can affect the K-capture behavior. Bituminous coal ash with high Al and Si contents are preferred as K-capture additive.
- Coal fly ash captures potassium from woody biomass more effectively than from straw (Cl-rich). Dosage of coal ash should be increased when firing herbaceous biomass containing Cl or S, like, straw.
- High-temperature can enhance the K-capture reaction by coal fly ash. Premixing fuel with coal fly ash and feed the mixture into boilers is preferred, since fully mixing and high temperatures can both be obtained.

Acknowledgements

This work is part of the project 'Flexible use of Biomass on PF fired power plants' funded by Energinet.dk through the ForskEL programme, Ørsted Bioenergy & Thermal Power A/S and DTU.

Appendix. Supplementary data

Appendix I: detailed information about quantification method of the K-capture reaction. Appendix II: detailed information about the equilibrium calculation. In Appendix II: part A is the detailed results of the equilibrium calculations of KCl capture by ASV2CFA0-32; Part B is the detailed results of the equilibrium calculations of K_2CO_3 capture by ASV2CFA0-32; Part C is the detailed results of the equilibrium calculations of K_2SO_4 capture by ASV2CFA0-32; Part D is the detailed results of the equilibrium calculations of KCl capture by AMVCFA0-32. Supplementary data to this article can be found online at https://doi.org/10.1016/j.fuproc.2019.05.038.

References

[1] H. Wu, P. Glarborg, F.J. Frandsen, K. Dam-Johansen, P.A. Jensen, Dust-firing of straw and additives: ash chemistry and deposition behavior, Energy Fuel 25 (2011) 2862–2873.
[2] S.V. Vassilev, D. Baxter, L.K. Andersen, C.G. Vassileva, An overview of the composition and application of biomass ash, Fuel 105 (2013) 19–39.
[3] J.M. Johansen, M. Aho, K. Paakkinen, R. Taipale, H. Egsgaard, J.G. Jakobsen, F.J. Frandsen, P. Glarborg, Release of K, Cl, and S during combustion and co-combustion with wood of high-chlorine biomass in bench and pilot scale fuel beds, Proc. Combust. Inst. 34 (2013) 2363–2372.
[4] S.V. Vassilev, D. Baxter, L.K. Andersen, C.G. Vassileva, T.J. Morgan, An overview of the organic and inorganic phase composition of biomass, Fuel 94 (2012) 1–33.
[5] S.V. Vassilev, D. Baxter, L.K. Andersen, C.G. Vassileva, An overview of the chemical composition of biomass, Fuel 89 (2010) 913–933.
[6] F.J. Frandsen, Ash Formation, Deposition and Corrosion When Utilizing Straw for Heat and Power Production, Department of Chemical and Biochemical Engineering, Technical University of Denmark, Denmark, 2011.
[7] Y. Laxminarayan, P.A. Jensen, H. Wu, F.J. Frandsen, B. Sander, P. Glarborg, Deposit shedding in biomass-fired boilers: shear adhesion strength measurements, Energy Fuel 31 (2017) 8733–8741.
[8] A.J. Damoe, P.A. Jensen, F.J. Frandsen, H. Wu, P. Glarborg, Fly ash formation during suspension firing of biomass: effects of residence time and fuel type, Energy Fuel 31 (2017) 555–570.
[9] L. Li, C. Yu, F. Huang, J. Bai, M. Fang, Z. Luo, Study on the deposits derived from a biomass circulating fluidized-bed boiler, Energy Fuel 26 (2012) 6008–6014.
[10] B. Anicic, W. Lin, K. Dam-Johansen, H. Wu, Agglomeration mechanism in biomass fluidized bed combustion – reaction between potassium carbonate and silica sand, Fuel Process. Technol. 173 (2018) 182–190.
[11] Y. Niu, H. Tan, Hui S e. Ash-related issues during biomass combustion: Alkali-induced slagging, silicate melt-induced slagging (ash fusion), agglomeration, corrosion, ash utilization, and related countermeasures, Prog. Energy Combust. Sci. 52 (2016) 1–61.
[12] A.J. Damoe, H. Wu, F.J. Frandsen, P. Glarborg, B. Sander, Impact of coal fly ash addition on combustion aerosols ($PM_{2.5}$) from full-scale suspension-firing of pulverized wood, Energy Fuel 28 (2014) 3217–3223.
[13] G. Wang, L. Shen, C. Sheng, Characterization of biomass ashes from power plants firing agricultural residues, Energy Fuel 26 (2012) 102–111.
[14] H.P. Nielsen, F.J. Frandsen, K. Dam-Johansen, L.L. Baxter, The implications of chlorine-associated corrosion on the operation of biomass-fired boilers, Prog. Energy Combust. Sci. 26 (2000) 283–298.
[15] H. Nielsen, Deposition of potassium salts on heat transfer surfaces in straw-fired boilers: a pilot-scale study, Fuel 79 (2000) 131–139.
[16] L.A. Hansen, H.P. Nielsen, F.J. Frandsen, K. Dam-Johansen, S. Hørlyck, A. Karlsson, Influence of deposit formation on corrosion at a straw-fired boiler, Fuel Process. Technol. 64 (2000) 189–209.
[17] Y. Zheng, A.D. Jensen, J.E. Johnsson, Deactivation of V_2O_5-WO_3-TiO_2 SCR catalyst at a biomass-fired combined heat and power plant, Appl. Catal. B Environ. 60 (2005) 253–264.
[18] Y. Zheng, A.D. Jensen, J.E. Johnsson, J.R. Thøgersen, Deactivation of V_2O_5-WO_3-TiO_2 SCR catalyst at biomass fired power plants: elucidation of mechanisms by lab- and pilot-scale experiments, Appl. Catal. B Environ. 83 (2008) 186–194.
[19] D. Lindberg, R. Backman, P. Chartrand, Thermodynamic evaluation and optimization of the (NaCl + Na_2SO_4 + Na_2CO_3 + KCl + K_2SO_4 + K_2CO_3) system, J. Chem. Thermodyn. 39 (2007) 1001–1021.
[20] M. Aho, P. Vainikka, R. Taipale, P. Yrjas, Effective new chemicals to prevent corrosion due to chlorine in power plant superheaters, Fuel 87 (2008) 647–654.
[21] K.O. Davidsson, L.E. Åmand, B.M. Steenari, A.L. Elled, D. Eskilsson, B. Leckner, Countermeasures against alkali-related problems during combustion of biomass in a circulating fluidized bed boiler, Chem. Eng. Sci. 63 (2008) 5314–5329.
[22] L. Wang, G. Skjevrak, J.E. Hustad, M. Grønli, Ø. Skreiberg, Effects of additives on barley straw and husk ashes sintering characteristics, Energy Procedia 20 (2012) 30–39.
[23] L. Wang, J.E. Hustad, Ø. Skreiberg, G. Skjevrak, M. Grønli, A critical review on additives to reduce ash related operation problems in biomass combustion applications, Energy Procedia 20 (2012) 20–29.
[24] L. Xu, J. Liu, Y. Kang, Y. Miao, W. Ren, T. Wang, Safely burning high alkali coal with kaolin additive in a pulverized fuel boiler, Energy Fuel 28 (2014) 5640–5648.
[25] B.M. Steenari, O. Lindqvist, High-temperature reactions of straw ash and the anti-sintering additives kaolin and dolomite, Biomass Bioenergy 14 (1998) 67–76.
[26] L. De Fusco, A. Boucquey, J. Blondeau, H. Jeanmart, F. Contino, Fouling propensity of high-phosphorus solid fuels: Predictive criteria and ash deposits characterisation of sunflower hulls with P/Ca-additives in a drop tube furnace, Fuel 170 (2016) 16–26.
[27] G. Wang, P.A. Jensen, H. Wu, F.J. Frandsen, B. Sander, P. Glarborg, Potassium Capture by Kaolin, part 1: KOH, Energy Fuel 32 (2018) 1851–1862.
[28] A. Fuller, Y. Omidiji, T. Viefhaus, J. Maier, G. Scheffknecht, The impact of an additive on fly ash formation/transformation from wood dust combustion in a lab-scale pulverized fuel reactor, Renew. Energy 136 (2019) 732–745.
[29] Y. Zheng, P.A. Jensen, A.D. Jensen, B. Sander, H. Junker, Ash transformation during co-firing coal and straw, Fuel 86 (2007) 1008–1020.
[30] D.C. Dayton, B.M. Jenkins, S.Q. Turn, R.R. Bakker, R.B. Williams, D. Belle-Oudry, L.M. Hill, Release of inorganic constituents from leached biomass during thermal conversion, Energy Fuel 13 (1999) 860–870.
[31] B.M. Jenkins, R.R. Bakker, J.B. Wei, On the properties of washed straw, Biomass Bioenergy 10 (1996) 177–200.
[32] S. Turn, C. Kinoshita, D. Ishimura, B. Jenkins, J. Zhou, Leaching of Alkalis in Biomass Using Banagrass as a Prototype Herbaceous Species, National Renewable Energy Laboratory, California, 2003.
[33] K.O. Davidsson, J.G. Korsgren, J.B.C. Pettersson, U. Jäglid, The effects of fuel washing techniques on alkali release from biomass, Fuel 81 (2002) 137–142.
[34] M. Oksa, P. Auerkari, J. Salonen, T. Varis, Nickel-based HVOF coatings promoting high temperature corrosion resistance of biomass-fired power plant boilers, Fuel Process. Technol. 125 (2014) 236–245.
[35] M.A. Uusitalo, P.M.J. Vuoristo, T.A. Mäntylä, High temperature corrosion of coatings and boiler steels below chlorine-containing salt deposits, Corros. Sci. 46 (2004) 1311–1331.
[36] H. Wu, M.S. Bashir, P.A. Jensen, B. Sander, P. Glarborg, Impact of coal fly ash addition on ash transformation and deposition in a full-scale wood suspension-firing boiler, Fuel 113 (2013) 632–643.
[37] Y. Zheng, P.A. Jensen, A.D. Jensen, A kinetic study of gaseous potassium capture by coal minerals in a high temperature fixed-bed reactor, Fuel 87 (2008) 3304–3312.
[38] Y. Liu, X. Duan, X. Cao, D. Che, K. Liu, Experimental study on adsorption of potassium vapor in flue gas by coal ash, Powder Technol. 318 (2017) 170–176.
[39] G. Wang, P.A. Jensen, H. Wu, F.J. Frandsen, B. Sander, P. Glarborg, Potassium capture by kaolin, part 2: K_2CO_3, KCl and K_2SO_4, Energy Fuel 32 (2018) 3566–3578.
[40] W.A. Punjak, M. Uberoi, F. Shadman, High-temperature adsorption of alkali vapors on solid sorbents, AICHE J. 35 (1989) 1186–1194.
[41] W.A. Punjak, F. Shadman, Aluminosilicate sorbents for control of alkali vapors during coal combustion and gasification, Energy Fuel 2 (1988) 702–708.
[42] K.-Q. Tran, K. Iisa, B.-M. Steenari, O. Lindqvist, A kinetic study of gaseous alkali capture by kaolin in the fixed bed reactor equipped with an alkali detector, Fuel 84 (2005) 169–175.
[43] M. Aho, E. Ferrer, Importance of coal ash composition in protecting the boiler against chlorine deposition during combustion of chlorine-rich biomass, Fuel 84 (2005) 201–212.
[44] G. Wang, P.A. Jensen, H. Wu, F.J. Frandsen, Y. Laxminarayan, B. Sander, P. Glarborg, KOH capture by coal fly ash, Fuel 242 (2019) 828–836.
[45] M. Izquierdo, X. Querol, Leaching behaviour of elements from coal combustion fly ash: an overview, Int. J. Coal Geol. 94 (2012) 54–66.
[46] A.G. Kim, G. Kazonich, M. Dahlberg, Relative solubility of cations in class F fly ash, Environ. Sci. Technol. 37 (2003) 4507–4511.
[47] R.S. Blissett, N.A. Rowson, A review of the multi-component utilisation of coal fly ash, Fuel 97 (2012) 1–23.
[48] S.V. Vassilev, C.G. Vassileva, A new approach for the classification of coal fly ashes based on their origin, composition, properties, and behaviour, Fuel 86 (2007) 1490–1512.
[49] M.S. Bashir, P.A. Jensen, F.J. Frandsen, S. Wedel, K. Dam-johansen, J. Wadenbäck, Suspension-firing of biomass. Part 2: boiler measurements of ash deposit shedding, Energy Fuel 26 (2012) 5241–5255.
[50] M.S. Bashir, P.A. Jensen, F.J. Frandsen, S. Wedel, K. Dam-johansen, J. Wadenbäck, S.T. Pedersen, Suspension-firing of biomass. Part 1: full-scale measurements of ash deposit build-up, Energy Fuel 26 (2012) 2317–2330.
[51] H. Wu, M.S. Bashir, P.A. Jensen, Full-Scale Ash Deposition Measurements at Avedøre Power Plant Unit 2 during Suspension-Firing of Wood with and without Coal Ash Addition, Technical University of Denmark, Denmark, 2012.